www.czasopisma.pan.pl PAN POLSKA AKADEMIA NAUK www.journals.pan.pl

Arch. Metall. Mater. **67** (2022), 1, 5-15

DOI: https://doi.org/10.24425/amm.2022.137466

S. DRZEWOWSKA[1*], TIAN-WEY LAN[2], B. ONDERKA[1]

THE INFLUENCE OF Ag_2Te ADDITION ON THERMOELECTRIC PROPERTIES OF BISMUTH TELLURIDE

The resistivity, Seebeck coefficient and thermal diffusivity were determined for $Bi_2Te_3 + Ag_2Te$ composite mixtures. Subsequent measurements were carried out in the temperature range from 20 to 270°C, and for compositions from pure Bi_2Te_3 to $x_{Ag_2Te} = 0.65$ selected along the pseudo-binary section of Ag-Bi-Te ternary system. It was found that conductivity vs. temperature dependence shows visible jump between 140 and 150°C in samples with highest Ag_2Te content, which is due to monoclinic => cubic Ag_2Te phase transformation. Measured Seebeck coefficient is negative for all samples indicating they are *n*-type semiconductors. Evaluated power factor is of the order $1.52 \cdot 10^{-3}$ and it decreases with increasing Ag_2Te content (at. %). Recalculated thermal conductivity is of the order of unity in W/(m K), and is decreasing with Ag_2Te addition. Finally, evaluated Figure of Merit is 0.43 at 100°C and decreases with temperature rise.

Keywords: thermoelectric materials; Seebeck coefficient; resistivity; thermal diffusivity; Bi_2Te_3-Ag_2Te system

Introduction

In 1821-3 Thomas Seebeck discovered [1] that when a closed circuit made of two different metals A and B is placed in the temperature gradient, this temperature difference produces a current flowing through the circuit. This phenomenon, called today Seebeck effect, was the first demonstration that the heat flux and the flow of electrons are coupled. When this circuit is broken, and the junctions between dissimilar metals are held at different temperatures, electric potential difference is produced between created this way terminals. Moreover, this voltage is proportional to the temperature difference imposed between two junctions. The proportionality constant is called Seebeck coefficient, and the whole effect can be described by the simple relation:

$$\Delta V = \alpha_{A/B} \Delta T \tag{1}$$

where ΔV is generated potential difference which is called thermoelectric force, ΔT is imposed temperature difference between two junctions, and $\alpha_{A/B}$ is Seebeck coefficient $(\Delta V/\Delta T)_{I=0}$ measured in Volts per Kelvin.

It is clear from eq. 1 that produced thermoelectric force ΔV depends not only on ΔT but also on $\alpha_{A/B}$, which in turn depends on a chosen material. The value of the coefficient α can be either positive or negative, depending on either holes or electrons conduction. Moreover, it depends also on the reference material. Usually metallic Pt is used as the reference in Seebeck coefficient determination. In such a case, the reference value is set to zero. Thus, to obtain the highest possible thermoelectric force from the source of heat, one must apply materials yielding highest value of Seebeck coefficient. Obviously, the heat (most important – waste heat) can be converted into electricity directly, and it is the reason why thermoelectric effect has attracted today so much attention. It can be exploited not only in thermocouples used in various temperature controlling devices, but also in large variety of other technological applications. Recent advances in this field as well as materials and their applications were described by Tritt and Subramanian [2], and Snyder and Toberer [3]. Numerous examples of technological applications can be mentioned, and some of them are given below. It appears that thermoelectric materials (TE) can be used in:

- converting the waste heat from vehicle exhaust into electric power [4],
- maintaining cathodic protection of oil drilling platforms [5],
- stabilizing operating wavelength of laser diodes [6],

[1] AGH UNIVERSITY OF SCIENCE AND TECHNOLOGY IN KRAKOW, FACULTY OF NON-FERROUS METALS, 30 MICKIEWICZA AVENUE, 30-059 KRAKOW, POLAND
[2] INSTITUTE OF PHYSICS, ACADEMIA SINICA, TAIPEI 11529, TAIWAN, ROC

* Corresponding author: sylwia.drzewowska@gmail.com

- recovering industrial waste-heat in aluminium smelting [7],
- powering space vehicles like Voyager and Cassini during NASA missions, as well as Curiosity rover on Mars [8,9]. For space missions electrical power was obtained by converting heat generated by ^{238}U isotope.

In order to optimize the performance of a thermoelectric material Abram Ioffe [10] developed the concept of dimensionless Figure of Merit, zT. It describes the maximum efficiency of a thermoelectric material for conversion of the heat flow into electricity, and is given by the following relation:

$$ZT = \frac{\alpha^2 \sigma T}{\kappa} \tag{2}$$

where α is Seebeck coefficient, σ is the electrical conductivity, κ is thermal conductivity (which is the sum of lattice and electronic contributions $\kappa_l + \kappa_e$), and T is the temperature. The higher value of zT one obtains, the better thermoelectric material it is.

It is clear from eq. (2) that maximization of zT requires materials with high electrical conductivity, large Seebeck coefficient and small thermal conductivity. These requirements are contradictory. High electrical conductivity is characteristic for metallic conductors, but experiments conducted with metallic thermocouples indicate that α is small (typically 10-60 μV/K). Thus, to increase Seebeck coefficient, a material with lower conductivity is required. It can happen if charge carriers are slow, or carrier concentration decreases. Theoretical considerations showed [11], that α depends not only on the number of carriers but also on their effective mass. Higher mass can be related to the density of states and energy band gap of a material. In general, α is proportional to energy per charge carrier, relative to Fermi level. Thus, it is dependent on temperature and electronic structure of the material. Mahan and Sofo [12] suggested that a good candidate for thermoelectric material is a narrow-bandgap semiconductor, for which the product $\alpha^2\sigma$ (called power factor) can be optimized by doping.

The numerator in eq. (2) is divided by thermal conductivity, which should be low to enhance zT. Since κ is determined by electrons (holes) as well as phonon movements, its low value is in conflict with the requirement for the material to exhibit high electronic conductivity. Fortunately, very low thermal conductivity may be achieved when crystal lattice is able to scatter phonons. Indeed, a kind of unusual material is needed to satisfy these requirements. Slack [13] suggested that "phonon-glass/electron-crystal" is needed for the best thermoelectric material.

It was found that materials possessing complex crystal structure may to a large extend separate the contribution of electrical conductivity from Seebeck coefficient, and also may decrease thermal conductivity [14,15]. From this point of view, scutterudites, clathrates, half-Heusler alloys and multicomponent chalcogenides are of interest [16]. Scattering phonons at interfaces at nanoscale is also being considered.

Bell [17] discussed the variety of future applications as well as changes in design of thermoelectric devices. To put these ideas into practice, one needs the thermoelectric material which assures $zT > 2$. Two routes of research were apparently exploited, which in general were based on the formation of nanostructures as well as mixing of various compounds accomplish this aim.

The results of those efforts have been analysed recently by Zabek and Morini [18], who gathered zT vs. T data for a large group of thermoelectric materials. These data, shown in Fig. 1, confirm that the increase of the Figure of Merit can be accomplished by either introduction of nanomaterials or by alloying.

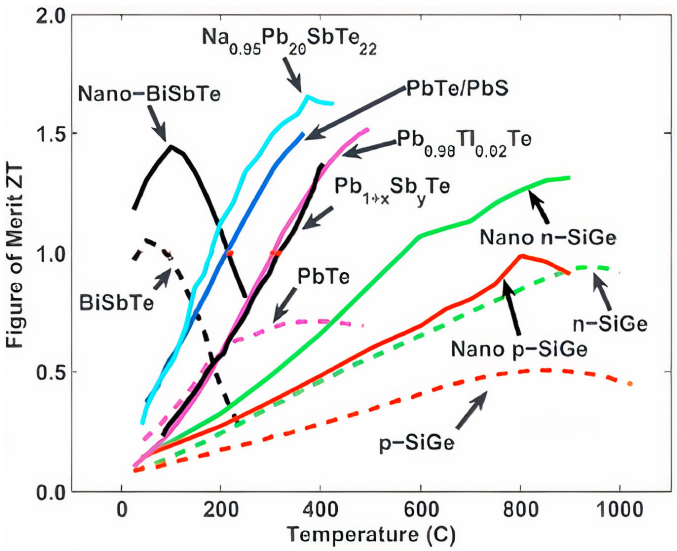

Fig. 1. Figure of Merit zT vs. temperature plot after Zabek and Morini [18]

In the past, the first thermoelectric material used by Goldsmid and Douglas in industrial application [19] was Bi_2Te_3. Bismuth telluride is n-type semiconductor with Seebeck coefficient –230 μV/K [20]. It has two-dimensional layered structure, which is rhombohedral-hexagonal. It was soon discovered that alloying Bi_2Te_3 with chalcogenides of antimony, lead tin, and germanium one can obtain even better thermoelectric material [21]. Unfortunately, ternary Pb-Ge-Se alloys with the highest Seebeck coefficient [20] contain lead and selenium which are considered to be toxic. Consequently, some alternatives were found which contain silver [22-24], copper [25-27]. For example, ternary chalcogenide $AgSbTe_2$ with GeTe addition (TAGS) has reached zT value above one [28].

Silver (I) telluride is itself an interesting electric material. Ag_2Te has three-dimensional monoclinic structure. At room temperature it is narrow band-gap semiconductor. As temperature increases it undergoes two phase transitions: monoclinic => α at 145°C, and α-fcc => β-bcc at 802°C. The first phase transition changes its transport properties into superionic conductor. Electronic properties of α- and β-Ag_2Te were investigated from room temperature to about 630ºC by Fujikane et al. [29]. They found that electrical resistivity changes at about 147ºC, i.e. around monoclinic => α transition. Calculated power factor suggests that it is better to use α-Ag_2Te as a thermoelectric material. Ouyang et al. [30] analysed thermal transport properties of α-Ag_2Te using molecular dynamic simulations. They found that

thermal transport in this phase results mainly from vibrations in Te^{2-} sublattice, while interactions between Ag^{+} and Te^{2-} ions hinder the heat transfer. It was also shown in that work [30] that stoichiometry of Ag_2Te compound has the influence on thermal conductivity. Silver deficient compound exhibits lower thermal conductivity. This study indicates directions one should take to lower thermal conductivity of a material. Selecting the crystal structure, controlling interactions between unlike ions and controlling stoichiometry by doping one have an influence on thermal conductivity. This is consistent with the theory of thermoelectricity summarized by Zhang and Zhao [31]. Ag_2Te is an important thermoelectric material due to its properties and therefore is combined with other thermoelectric materials that can increase the *zT* factor.

Another factor which can be varied is the size. Lee et al. [32] investigated thermoelectric properties of synthesized single crystalline Ag_2Te nanowires. They observed that when Ag_2Te phase changes into cubic structure, power factor suddenly decreases. It suggests the increased density of states of electrons due to the nanowire structure. It seems that silver (I) telluride is an interesting material which can be used in thermoelectrics. However, some attempts have been made to mix it with other thermoelectric materials based on bismuth telluride. For example Lee et al. [33] investigated thermoelectric properties of $Bi_{0.5}Sb_{1.5}Te_3/Ag_2Te$ bulk composites with size- and shape-controlled Ag_2Te nano-particles dispersion, Sakakibara et al. [34,35] measured thermoelectric properties for $AgBiTe_2$-Ag_2Te composites, Fang et al. [36] investigated thermoelectric properties of silver telluride-bismuth telluride nanowire heterostructure. Since the influence of Ag_2Te addition on thermoelectric properties of Bi_2Te_3 has not been reported so far, it was decided to investigate thermoelectric properties of alloys in Ag_2Te – Bi_2Te_3 pseudo-binary system. Thus, the aim of this paper is to measure the resistivity (reciprocal conductivity), Seebeck coefficient and thermal diffusivity, and then to determine power factor and the Figure of Merit *zT* of Ag_2Te-Bi_2Te_3 alloys as a function of temperature and alloy composition.

Materials and experimental methods

Samples of Ag-Bi-Te alloys were synthesized by using SPS method. Powders of Bi_2Te_3 (99.98% pure, obtained from Alfa Aesar) and Ag_2Te (obtained from Sigma Aldrich) were grinded first in the ball mill (Fritsch, Pulverisette 23, the container and balls made of ZrO_2). This procedure equalized diameters of grains of the initial materials before their mixing. Next, the alloy samples with the compositions given in Tab. 1 were prepared by mixing these powders. Compositions of six alloys were selected along the pseudo-binary section Ag_2Te-Bi_2Te_3 of the ternary Ag-Bi-Te system.

Prepared samples were introduced into sintering apparatus Dr Sinter, Spark Plasma Sintering System, model SPS – 515S, SPS Syntex Inc. (Kanagawa, Japan). The powders were placed into graphite die (d = 10 mm, h = 3 mm). Before powder introduction, a graphite disc was placed on the bottom of the matrix to separate the powder from the press piston. Similar disc was placed from above to cover the powder. The sintering took 5 min at the temperature 400°C and under pressure of 50 MPa. The rate of heating was set to 50°C/min. After sintering samples were analysed by X-ray to check their final phase composition. The phase composition of studied alloys was determined by X-ray Powder Diffraction (XRD) method using Rigaku Japan MiniFlex II X-ray Diffractometer with Cu-Kα radiation. Next, to check stability of prepared samples, small portion of each was subjected to TGA analysis. These experiments were conducted on Netzsch

TABLE 1

Composition of Ag-Bi-Te alloys along the pseudo-binary section Ag_2Te-Bi_2Te_3 of the ternary Ag-Bi-Te system, mole fractions of Ag_2Te and Bi_2Te_3 compound in the samples and experimental results (XRD data) for prepared samples

No Sample	Sample composition [at. %]	x_{Ag_2Te}	$x_{Bi_2Te_3}$	XRD results	
				Phase	No. chart
1	Bi40Te60	0	1	Bi_2Te_3	00-015-0863
				Bi_2Te_3	00-010-0054
				Bi_2Te_3	01-076-2813
2	Ag05Bi37Te58	0.119	0.881	Bi_2Te_3	01-076-2813
				Ag_2Te	01-081-1985
3	Ag10Bi34Te56	0.227	0.773	Bi_2Te_3	01-085-0439
				Ag_2Te	01-081-1985
4	Ag17.5Bi29.5Te53	0.372	0.628	Bi_2Te_3	00-015-0863
				Ag_2Te	01-081-1985
				$Ag_{1.85}Te$	00-018-1186
5	Ag25Bi25Te50	0.500	0.500	Bi_2Te_3	00-015-0863
				Ag_2Te	00-034-0142
				$AgBiTe_2$	01-076-6580
6	Ag35Bi19Te46	0.648	0.352	$AgBiTe_2$	00-018-1172
				Bi_2Te_3	00-015-0863
				Ag_2Te	01-081-1985
				$Ag_{1.85}Te$	00-018-1186

STA 449 F3 (Germany) apparatus with the 20 deg/min heating rate. No weight loss of investigated samples up to 350°C was detected. Finally, after synthesis, samples were polished and their density was determined from their mass and the volume of water displaced by the sample (Archimedes' principle).

Samples for thermoelectric properties measurements were prepared from samples obtained by SPS method. Small cuboids of dimensions $l = 10$ mm, $w = 2.8$-3.0 mm and $h = 0.9 - 1.55$ mm were cut off from sintered samples. Determination of resistivity ρ and Seebeck coefficient α was conducted on ZEM-3, ULVAC Co. Ltd (Japan) apparatus. In order to measure the resistivity and Seebeck coefficient, the investigated sample is placed between the upper and lower blocks in the heating furnace. The heater in the lower block provides the temperature gradient. In this off-axis four point geometry, thermocouples are pressed against the side of the sample, and they measure T_1 and T_2 temperatures at two different points (i.e. they establish temperature gradient ΔT). The surface of the samples was carefully polished to assure good thermal and electrical contacts. The voltage difference between two alike wires of these two thermocouples is measured yielding thermoelectric force ΔV. Experiments were carried out in the temperature range from 20 to 270°C under helium at the pressure 10^{-1} MPa. Temperature was varied in steps of 20 degree, and measurements were taken when selected temperature difference was attained before each measurement. The device is operating in a steady-state mode in which measurements are taken after stabilization of the temperature gradient. Voltage drop E is measured at the same two points of the sample and between the same alike thermocouple wires. After correcting this voltage drop for thermoelectric force ΔV generated by temperature gradient, the resistance of the sample can be determined. Having the distance between tips of these two thermocouples and the sample geometry, specific resistivity (conductivity) can be derived. In this way both, Seebeck coefficient and resistivity of the sample were determined.

Thermal diffusivity D_T (in cm^2/s) was determined by using laser flash method with the apparatus Netzsch LFA 457 (Germany). In this experimental setup the thin sample (about 10 mm in diameter and 1-2 mm in thickness) is exposed to the short laser pulse (pulse energy 5 to 8 J) from the bottom, while its temperature is monitored from above by an infrared (IR) detector. The sample is placed in thermal shield to eliminate radial heat losses, and to assure one-dimensional heat flow. The pulse of energy is absorbed by the sample's surface, and the temperature change of the sample versus time is recorded on the other side of the sample to determine its maximum rise. Parker et al. [37] developed the model which does not require the knowledge of received energy pulse. Assuming adiabatic case, thermal diffusivity is proportional to the ratio ($l^2/t_{½}$), where $t½$ is the time necessary for the temperature to rise to ½ of its maximum. Parker's model was later improved by Cowan [38], who took into account heat losses due to radiation and convection on the surface. This correction has been implemented in the software operating with the device. The whole experimental setup is placed in a furnace to carry on measurements at different temperatures. Obtained data on the heat diffusivity can be converted into thermal conductivity κ (in W/cm K) with help of the relation [39]:

$$\kappa = D_T \, d \, C_p \tag{3}$$

where d is density [g/cm^3] and C_P is specific heat capacity of the sample in J /g K.

The microstructure of selected sintered samples was observed by scanning electron microscopy (SEM) (Hitachi, SU-70, Japan, with electron microprobe ThermoScientific, with ZAF correction). For qualitative and quantitative analysis the EDX (Energy Dispersive X-ray Spectroscopy) method was applied.

Results

The results of experimentally determined densities of respective samples are shown in Fig. 2, in which they are compared with theoretical density.

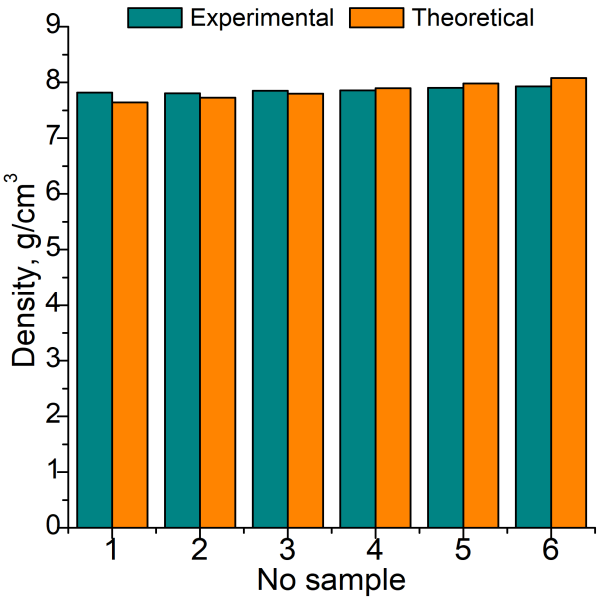

Fig. 2. Bar graph of determined samples density as compared with its theoretical values. (For representation of the references to colour in this figure legend, the reader is referred to the web version of this article)

It may be seen that the maximum difference between theoretical and measured densities is (at average) of the order of 2% which fit in the experimental error range.

Results of X-ray analysis of the samples 1-6 prepared for subsequent measurements are shown in Fig. 3, while the results of this analysis are given in Table 1. Obtained results indicate that two-phase mixture was obtained for all samples. Additionally, new ternary phase $AgBiTe_2$ is also identified in samples rich in Ag_2Te.

However, it must be mentioned that this phase is not present on the microstructure revealed by SEM and shown in Fig. 4.

The results of resistivity measurements were recalculated to obtain specific conductivity ($\sigma = 1/\rho$), which is shown in Fig. 5 as a function of temperature for different sample composition.

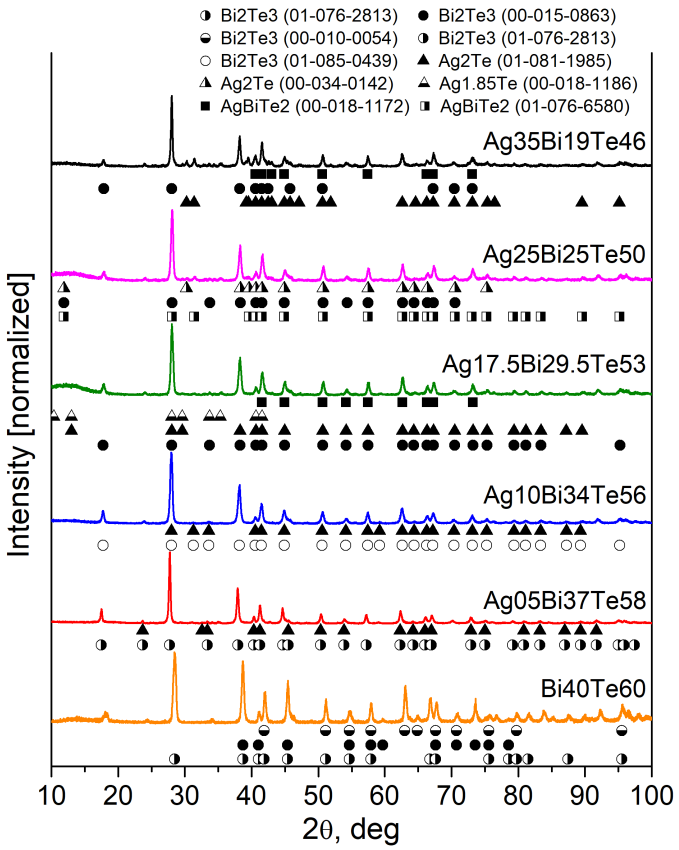

Fig. 3. X-ray powder spectra obtained for samples 1-6: a) no. 1 – Bi40Te60, b) no. 2 – Ag05Bi37Te58, c) no. 3. – Ag10Bi34Te56, d) no. 4 – Ag17.5Bi29.5Te53, e) no. 5 – Ag25Bi25Te50, f) no. 6 – Ag35Bi19Te46. (For representation of the references to colour in this figure legend, the reader is referred to the web version of this article)

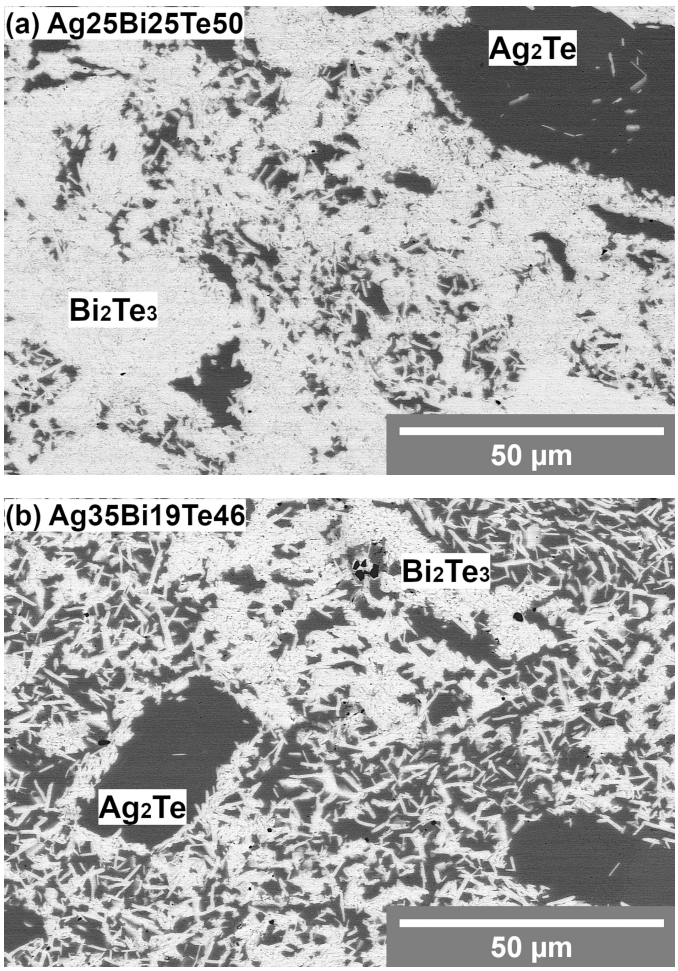

Fig. 4. Microstructures of the alloys Ag_2Te-Bi_2Te_3 sintered alloys at 400°C and under pressure of 50 MPa corresponding to: (a) the sample no. 5, (b) the sample no. 6 obtained by SEM Hitachi, SU-70 with ×1000 magnification

In the range 140-150°C the change in slope of this dependence is visible. This change is getting more pronounced with the increasing Ag_2Te content. It indicates the detection of the structural transformation of Ag_2Te which according to the binary Ag-Te phase diagram [40] is equal to 145°C.

Similarly, Seebeck coefficient determined for different samples is shown as a function of temperature in Fig. 6.

Obtained values of the coefficient are negative for all samples which means they are *n*-type semiconductors. The value measured for Bi_2Te_3 is almost constant with temperature. The addition of Ag_2Te results in visible decrease of the coefficient (it roughly corresponds to doped Bi_2Te_3 around room temperature). It is also seen that the temperature increase results in the reduction of Seebeck coefficient towards more positive values.

Having determined Seebeck coefficient and the conductivity, the power factor ($\sigma \cdot \alpha^2$) was derived for two temperatures 100 and 262°C. These results are shown in Fig. 7 as a function of a sample composition. In general, increasing the Ag_2Te content reduces the power factor, while the increase of temperature has small effect on this change. The maximum value of the power factor determined in this study is $1.52 \cdot 10^{-3}$ at 100°C and $0.77 \cdot 10^{-3}$ at 262°C. This result is encouraging since to be applied in current devices, TE material should have the power factor of the order of 10^{-3}.

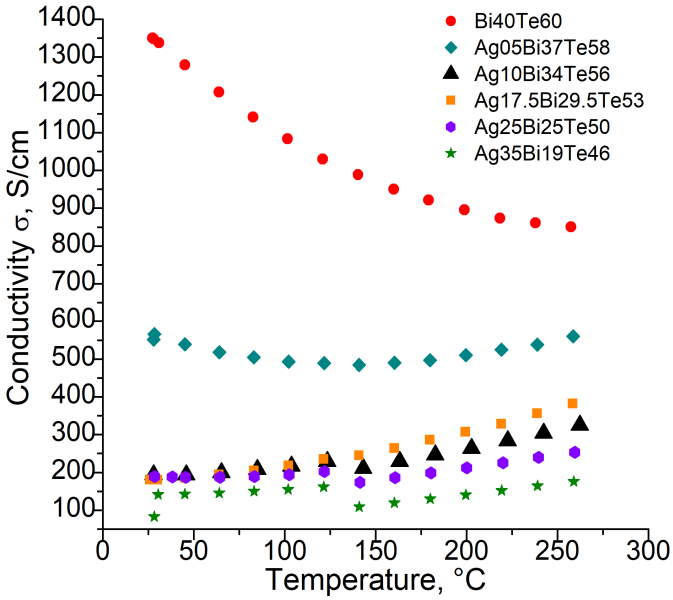

Fig. 5. Conductivity vs. temperature plots for samples 1-6: a) no. 1 – Bi40Te60, b) no. 2 – Ag05Bi37Te58, c) no. 3. – Ag10Bi34Te56, d) no. 4 – Ag17.5Bi29.5Te53, e) no. 5 – Ag25Bi25Te50, f) no. 6 – Ag35Bi19Te46

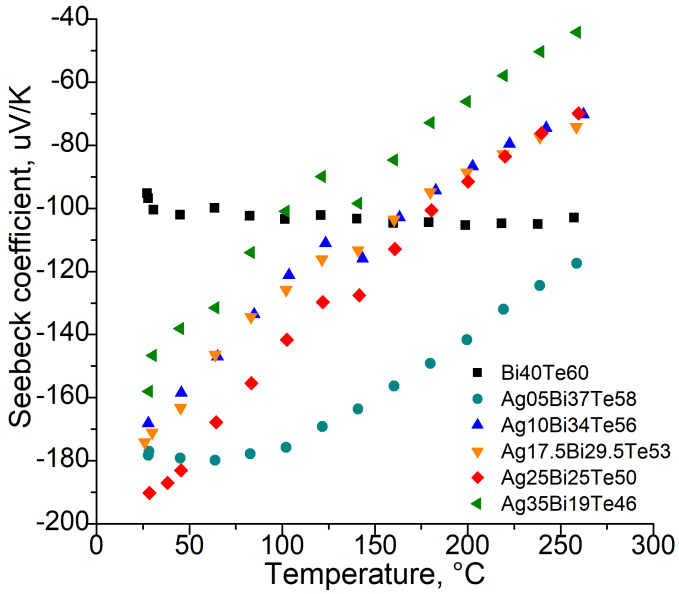

Fig. 6. Seebeck coefficient vs. temperature plots for samples 1-6: a) no. 1 – Bi40Te60, b) no. 2 – Ag05Bi37Te58, c) no. 3. – Ag10 Bi34Te56, d) no. 4 – Ag17.5Bi29.5Te53, e) no. 5 – Ag25Bi25Te50, f) no. 6 – Ag35Bi19Te46

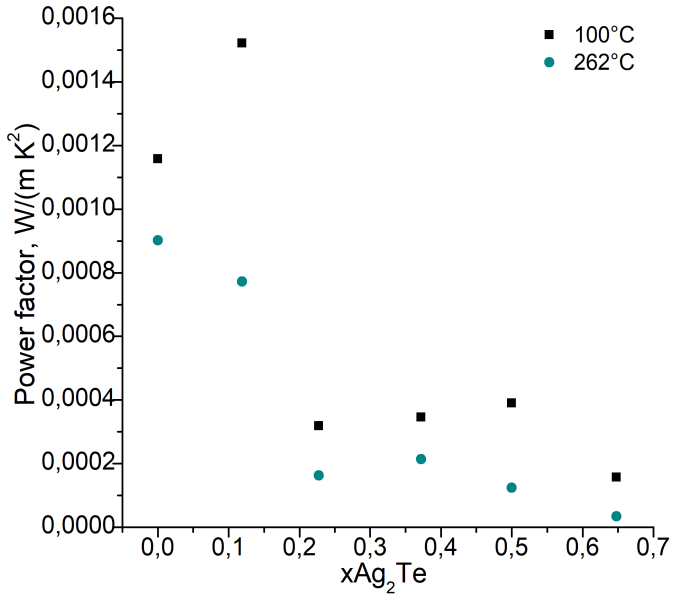

Fig. 7. Power factor vs. sample composition evaluated at two temperatures 100 and 262°C

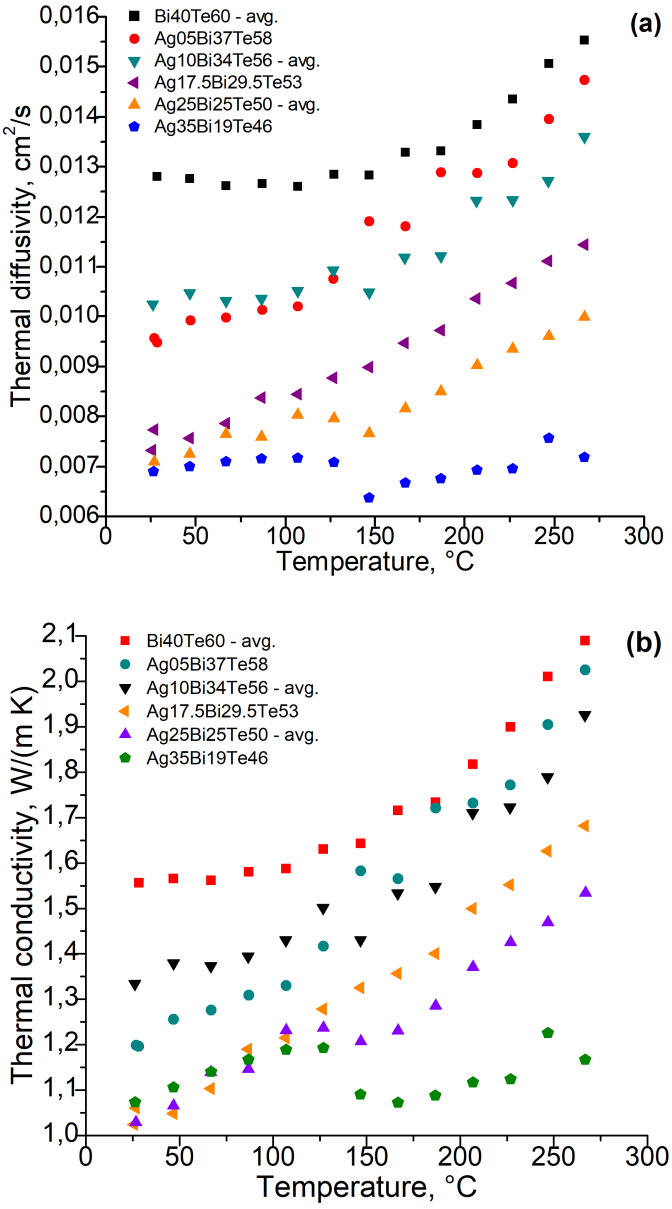

Fig. 8. Thermal diffusivity a) and recalculated thermal conductivity b) for samples 1 – 6 as a function of temperature. No. 1 – Bi40Te60, no. 2 – Ag05Bi37Te58, no. 3. – Ag10Bi34Te56, no. 4 – Ag17.5Bi29.5Te53, no. 5 – Ag25Bi25Te50, no. 6 – Ag35Bi19Te46

In order to obtain thermal conductivity, thermal diffusivity was measured and obtained results are shown in Fig. 8a. Next, they were recalculated using eq. 3. Density of respective samples was taken from this work. To calculate specific heat capacity, heat capacity data for Bi_2Te_3 and Ag_2Te were accepted after Kubaschewski, Alcock and Spencer [41]. The results of thermal conductivity calculations are shown in Fig. 8b.

It is obvious that the addition of Ag_2Te decreases thermal diffusivity, which however increases with temperature. This trend is observed for all samples. Moreover, there is a change in slope of this dependence which may suggest some changes in heat transfer mechanism. As far as thermal conductivity is concerned, it decreases with the silver telluride addition. The slope of temperature dependence increases with rising temperature. The jump resulting from phase transformation of Ag_2Te is also visible for alloys with highest Ag_2Te content.

Finally, the Figure of Merit, zT, was calculated and is shown in Fig. 9 for two temperatures 100 and 265ºC as a function of the sample composition.

In turn, the dependence of the Figure of Merit on temperature is shown in Fig. 10.

It appears that increasing the temperature one can slightly reduce the Figure of Merit. It changes irregularly with Ag_2Te addition reaching maximum value 0.43 at 100°C, and 0.2 at 262°C (Fig. 9).

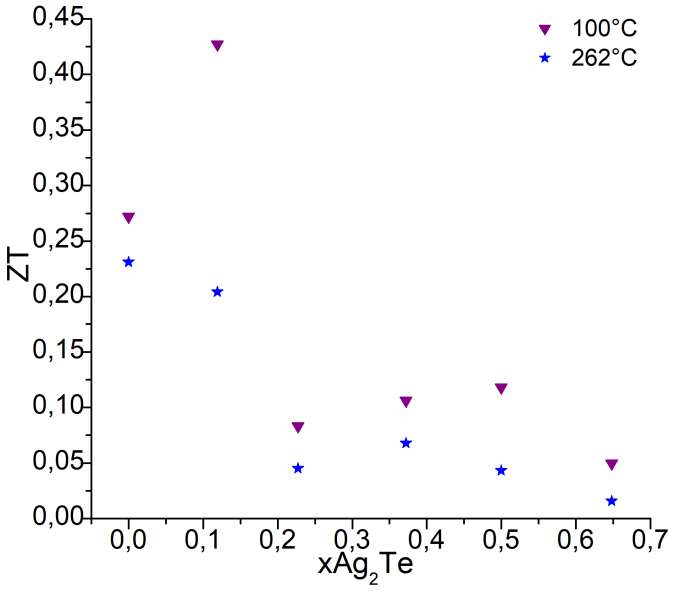

Fig. 9. Figure of Merit vs. sample composition evaluated at two temperatures 100 and 262°C

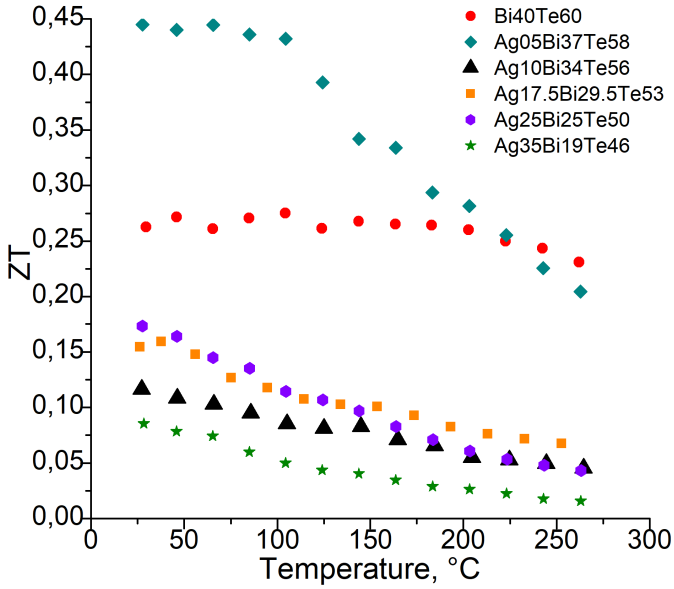

Fig. 10. Figure of Merit vs. temperature evaluated for samples 1 – 6. No. 1 – Bi40Te60, no. 2 – Ag05Bi37Te58, no. 3. – Ag10Bi34Te56, no. 4 – Ag17.5Bi29.5Te53, no. 5 – Ag25Bi25Te50, no. 6 – Ag35 Bi19Te46

Discussion of experimental data

The very detailed analysis of possible experimental difficulties in thermoelectric transport properties measurements has been given recently by Borup et al. [42]. Thus, in this paper we are going to concentrate only on several points directly related to our experiments. The first requirement to obtain reliable results on thermoelectric properties of a material is careful sample preparation. Since Seebeck coefficient is sensitive to the presence of impurities, the purity of starting materials is of great importance. We used commercially available Bi_2Te_3 and Ag_2Te, which were 99. 98% and 99% pure, respectively. Thus, introduction of some impurities into a final sample cannot be excluded. Application of SPS method of the sample synthesis gave product which after synthesis had density differing from theoretical density by about 2%. It is reasonable result, since it is in the range of deviations in which determined zT value is still acceptable [43]. However, as a result of high-temperature synthesis, X-ray detected in samples a fraction of a new phase $AgBiTe_2$. It indicates the formation of a three-phase mixture, which apparently must affect the electronic properties of the product. The stoichiometry of this phase is identical with $AgSbTe_2$ and $AgBiSe_2$, which are known to exhibit good thermoelectric properties [29,44-46]. However, the stability and the range of existence of $AgBiTe_2$ is not so clear. Pseudo-binary Ag_2Te-Bi_2Te_3 section [47] of the ternary Ag-Bi-Te phase diagram indicates that this phase is stable only in narrow temperature range, i.e. from eutectoid reaction at 443ºC to congruent melting between 555°C [48] and 557ºC [49]. Thus, in the temperature range of our experiments it should not exist. Its presence is probably due to the nonequilibrium conditions during synthesis and it is metastable. Such a conclusion is supported by SEM analysis (Fig. 4) which did not revealed the presence of this ternary phase in the samples corresponding to their composition. Their controversy can be solved when careful investigations of phase equilibria in the ternary system Ag-Bi-Te will be conducted. At this moment it can be only speculated that presence detected by X-ray analysis has something to do with temperature, pressure or time of samples synthesis. Thus, either the reaction has not been completed (too short time), or fast decomposition of this phase took place. It would be very interesting to isolate this phase and to determine its thermoelectric properties. Its small range of stability could hinder this kind of experiment. However, alloying of $AgBiTe_2$ with another phases was conducted. For example, Sakakibara et al. [34,35] mixed $AgBiTe_2$ and Ag_2Te, synthesized by traditional melting method and carried out the measurements of the thermoelectric properties for these composites. Avramova and Plachkova [50] tested electrical resistivity for thermoelectric materials in the GeTe-$AgBiTe_2$ system. Tan et al. [51] combined SnTe and $AgBiTe_2$ compounds by melting and SPS methods and measured Seebeck coefficient, electrical conductivity, thermal conductivity and Hall mobility.

Measurements of resistivity and Seebeck coefficient were carried out simultaneously on a commercial setup. In their recent work de Boor and Muller [52] analyzed the errors committed most often during Seebeck coefficient determination. They pointed out that the main sources of errors are thermal contacts resistances, heat flux through thermocouples, but also the way how Seebeck coefficient is extracted from the raw data recorded during experiments. Simultaneous acquisition of the measured temperature and voltages also matters since there can be an interference from the heaters. In case of commercial equipment those problems depend on the construction of the device, data acquisition system and operating software. ZEM-3 has its own software provided with the apparatus. Thus, from the point of view of the experimenter, the greatest care must be taken during sample preparation (surface, dimensions) since the mode

of device's operation is fixed by the software. It should be only mentioned that in case of data comparison, reference material must be also taken into account. In our case it is constantan, while table's values are usually given against Pt. In turn, the main error in the resistivity measurements seems to result from small differences in samples dimensions and quality of electrical contacts. These samples are small and it is difficult to make them identical. Also, non-homogeneity of sintered samples and their density may influence measured resistivity. Obtained results indicate Ag_2Te phase transition, which is visible in the range 140-150°C. It corresponds to monoclinic => cubic transformation [40], and the change in slope of conductivity σ vs. temperature T dependence is more visible as Ag_2Te content increases.

Seebeck coefficient measured for Bi_2Te_3 is negative and slightly decreasing with temperature. This trend of Seebeck coefficient is comparable to the trend of the curves for the plot of the Seebeck coefficient as a function of temperature in the work of Kim and Mitani [53]. Bi_2Te_3 samples were fabricated using hot pressing method [53]. In Kim and Mitani's work [53] the values of the Seebeck coefficient are in the range of about –140 to –150 μV/K for the temperature range 0-27 °C. The values of the Seebeck coefficient in this work are in the range between –95 and –105 μV/K for the temperature range of 0-300°C. The obtained values of the Seebeck coefficient are relatively comparable, taking into account the differences in the methods of sample synthesis, the grain size of the materials. The sample of pure Bi_2Te_3 was made of commercially available reagent and a possible influence from impurities is not known. However, large negative values of Seebeck coefficient can be observed at low temperature with Ag_2Te additions. This effect changes slightly with increasing temperature and simultaneous increase of electrical conductivity. At high temperature, silver telluride becomes superionic conductor and the change in conduction mechanism is possible. Moreover, silver telluride and Bi_2Te_3 react forming intermetallic phase $AgBiTe_2$ [49]. Though this phase is supposed not to exist below 443°C, its presence in samples is confirmed by X-ray studies. Unfortunately, thermophysical properties of this phase are not known and it's hard to predict its influence on measured Seebeck coefficient.

Thermal conductivity was derived indirectly from measured thermal diffusivity and specific heat capacity calculated from thermochemical tables [41]. While linear approximation should work well for the mixture of two phases, the presence of $AgBiTe_2$ phase of unknown C_p must affect the value of C_p for the mixture. Thermal conductivity can be determined directly by e.g. DSC or drop calorimetry. However, this approach requires additional measurements on the same sample. It may be difficult since requirements of these two experiments can be quite different as far as dimensions of samples are concerned. There is another method based on LFA apparatus which makes use of maximum temperature rise, T_{max}, related to C_p by the relationship:

$$C_p = \frac{Q}{m T_{max}} \tag{4}$$

where Q is a heat, m is a mass. It requires however accurate determination of the amount of heat Q absorbed by the sample. And it is not so obvious. This problem can be solved by the proper calibration with a material with well-known specific heat [54]. However, we used indirect method which may be acceptable if the sample consists of the mixture of two phases having well-known specific heat capacity. In our system this condition is almost fulfilled, but the presence of the ternary phase (its amount is not known) certainly introduces an error in final C_p estimation.

Finally, power factor (which defines electrical performance of thermoelectric materials) and Figure of Merit (indicating maximum efficiency of TE material) has been evaluated (Fig. 9, 10). The maximum power factor found in this study is $1.52 \cdot 10^{-3}$ at 100°C, and maximum Figure of Merit is of the order of 0.43 at 100°C. Our findings are compatible with the results of Chen et al. [24] who studied a silver alloyed *n*-type Bi_2Te_3. They showed that the addition of Ag nanoparticles to Bi_2Te_3 nanopowder yields TE material with a Figure of Merit of 1.48 at room temperature. Thus, the reduction of the size of particles increased the Figure of Merit above 1.0 [24]. However, it is one of two studies of thermoelectric properties we found for Ag-Bi-Te alloys. In a second research, Fang et al. [36] investigated thermoelectric properties of silver telluride-bismuth telluride nanowire heterostructure. However, the research focused on the thermoelectric properties of nanomaterials and it is difficult to compare them with the properties of bulk materials. Moreover, two chemical compositions of the samples were investigated: 4.4 mol% and 15.2 mol% Bi_2Te_3 for the first and the second sample, respectively [36]. Therefore, there is no aspect to compare with this work. Whereby, the comparison with other data obtained for Ag-Bi-Te system is not possible at present.

A decrease of the zT values is observed with the temperature increase in Fig. 10. The Figure of Merit values for pure Bi_2Te_3 are in the range of 0.23-0.27, which is quite a low result for this material. Bi_2Te_3 alloys, which are prepared by traditional zone melting method, have got zT factor close to 0.8-1 [55,56]. Tang et al. [57] prepared Bi_2Te_3 bulk material with a layered structure by the melt-spinning and SPS processes and a maximum zT of 1.35 was obtained at room temperature [57]. The zT values are influenced by the Seebeck coefficient which depends on the concentration of the charge carriers. It has been observed that various methods of Bi_2Te_3 synthesis can cause to increase of electrically active defects in the polycrystalline form, which may be caused by charged defects at the non-equilibrium grain boundary or by expanded defects or unknown impurities [58]. For example, high energy ball milling [59,60] may have a donor-like effect. Annealing or other high temperature treatment (e.g. plasma spark sintering [59,61]) may reduce, but may not eliminate, the doping effect. In the materials fabricated in this way, the concentration of the charge carrier may change significantly, and as a consequence even cause the reversal of the dominant type of the charge carrier in relation to the growing composition [62,63]. Therefore, the applied methods of synthesis in this work might have an influence on the values of the Seebeck coefficient of the Bi_2Te_3 compound as well as Ag-Bi-Te alloys, and thus on the values of the zT factor.

Conclusions

Summarizing the results of this work the following conclusions can be drawn:

- The Seebeck coefficient, resistivity, thermal conductivity, power factor and Figure of Merit zT of selected alloys in the Ag_2Te-Bi_2Te_3 pseudo-binary system were investigated for the first time.
- Up to 270°C all prepared samples consist of the mixture of two phases: Bi_2Te_3+Ag_2Te. For increasing amount of Ag_2Te the presence of ternary phase $AgBiTe_2$ becomes visible.
- Both initial components of these mixtures are *n*-type semiconductors. Above around 150°C in samples richer in Ag_2Te, conductivity exhibits jump due to the phase transformation, and slightly increases with temperature due to the change in charge transfer mechanism. Only in case of commercial Bi_2Te_3 a slow, steady decrease in conductivity with temperature is observed.
- Thermal conductivity increases with Ag_2Te addition, while the increase of temperature slightly accelerates this increase.
- The maximum power factor is of the order $1.52 \cdot 10^{-3}$ at 100°C and Figure of Merit is 0.43 at 100°C, and both parameters decrease with temperature.
- The study of phase equilibria in Ag-Bi-Te ternary system is necessary to assess the range of existence and the stability of respective phases. It is desirable to establish the temperature and composition range in which solid solutions and intermetallic phases may exist.

Acknowlegdement

This work was carried out in the framework of Polish-Taiwanese cooperation under grant DKO/PL-TW1/5/2013 “Phase Diagram Determination of Thermoelectric Materials”. One of us (S.D.) is grateful to Prof. Sinn-Wen Chen from National Tsing Hua University and Dr. Yang-Yuan Chen from Institute of Physics, Academia Sinica in whose laboratory this experimental work was carried out.

REFERENCES

[1] T.J. Seebeck, Magnetische Polarisation der Metalle und Erze dürch Temperatur-Differenz, Abhandlungen der Königlichen Akademie des Wissenschaften, Berlin 265-373 (1822-1823). https://collections.thulb.uni-jena.de/rsc/viewer/HisBest_derivate_00003304/NT_189_Seite_004.tiff

[2] T.M. Tritt, M.A. Subramanian, Thermoelectric Materials, Phenomena, and Applications: A Bird’s Eye View, MRS Bull. **31** (3), 188-198 (2006). DOI: https://doi.org/10.1557/mrs2006.44

[3] G.J. Snyder, E.S. Toberer, Complex thermoelectric materials, Nat. Mater. **7** (2), 105-114 (2008). DOI: https://doi.org/10.1038/nmat2090

[4] K. Ikoma, M. Munekiyo, K. Furuya, M. Kobayashi, T. Izumi, K. Shinohara, Thermoelectric module and generator for gasoline engine vehicles, Seventeenth Internat. Conf. Thermoelectr. Proc. ICT98 (Cat. No.98TH8365), 1998, 464-467. DOI: https://doi.org/10.1109/ICT.1998.740419

[5] https://www.farwestcorrosion.com/thermoelectric-generators-for-cathodic-protection-by-gentherm.html

[6] http://www.marlow.com/products.html

[7] T. Hendricks, W.T. Choate, Engineering scoping study of thermoelectric generator systems for industrial waste heat recovery, EERE Publication and Product Library 2006. DOI: https://doi.org/10.2172/1218711

[8] J. Yang, T. Caillat, Thermoelectric materials for space and automotive power generation, MRS Bull. **31** (3), 224-229 (2006). DOI: https://doi.org/10.1557/mrs2006.49

[9] http://thermoelectrics.matsci.northwestern.edu/

[10] A. F. Ioffe, Semiconductor thermoelements, and thermoelectric, Cool. Infosearch Ltd., 1957.

[11] M. Cutler, J.F. Leavy, R.L. Fitzpatrick, Electronic transport in semimetallic cerium sulfide, Phys. Rev. **133** (4A), A1143-A1152 (1964). DOI: https://doi.org/10.1103/PhysRev.133.A1143

[12] G.D. Mahan, J.O. Sofo, The best thermoelectric, Proc. Natl. Acad. Sci. USA **93** (15), 7436-7439 (1996). DOI: https://doi.org/10.1073/pnas.93.15.7436

[13] G. Slack, CRC Handbook of Thermoelectrics. Boca Raton, FL: CRC Press, 1995.

[14] L.D. Hicks, M.S. Dresselhaus, Effect of quantum-well structures on the thermoelectric figure of merit, Phys. Rev. B **47** (19), 12727-12731 (1993). DOI: https://doi.org/10.1103/PhysRevB.47.12727

[15] J.M.O. Zide, D. Vashaee, Z.X. Bian, G. Zeng, J. E. Bowers, A. Shakouri, A.C. Gossard, Demonstration of electron filtering to increase the Seebeck coefficient in $In_{0.53}Ga_{0.47}As/In_{0.53}Ga_{0.28}Al_{0.19}As$ superlattices, Phys. Rev. B **74** (20), 205335-1-205335-5 (2006). DOI: https://doi.org/10.1103/PhysRevB.74.205335

[16] G.S. Nolas, J. Poon, M. Kanatzidis, Recent developments in bulk thermoelectric materials, MRS Bull. **31** (3), 199-205 (2006). DOI: https://doi.org/10.1557/mrs2006.45

[17] L.E. Bell, Cooling, heating, generating power, and recovering waste heat with thermoelectric systems, Science **321** (5895) 1457-1461 (2008). DOI: https://doi.org/10.1126/science.1158899

[18] D. Zabek, F. Morini, Solid state generators and energy harvesters for waste heat recovery and thermal energy harvesting, Therm. Sci. Eng. Prog. **9**, 235-247 (2019). DOI: https://doi.org/10.1016/j.tsep.2018.11.011

[19] H.J. Goldsmid, R.W. Douglas, The use of semiconductors in thermoelectric refrigeration, Brit. J. Appl. Phys. **5** (11), 386-390 (1954). DOI: https://doi.org/10.1088/0508-3443/5/11/303

[20] https://www.electronics-cooling.com/2006/11/the-seebeck-coefficient/

[21] C. Wood, Materials for thermoelectric energy conversion, Reports Prog. Phys. **51** (4), 459-539 (1988). DOI: https://doi.org/10.1088/0034-4885/51/4/001

[22] J. Yang, R. Chen, X. Fan, S. Bao, W. Zhu, Thermoelectric properties of silver-doped n-type Bi_2Te_3-based material prepared by mechanical alloying and subsequent hot pressing, J. Alloys Compd. **407** (1-2), 330-333 (2006). DOI: https://doi.org/10.1016/j.jallcom.2005.06.041

[23] Q. Zhang, X. Ai, L. Wang, Y. Chang, W. Luo, W. Jiang, L. Chen, Improved thermoelectric performance of silver nanoparticles-dispersed Bi_2Te_3 composites deriving from hierarchical two-phased heterostructure, Adv. Funct. Mater. **25** (6), 966-976 (2015). DOI: https://doi.org/10.1002/adfm.201402663

[24] S. Chen, N. Logothetis, L. Ye, J. Liu, A high performance Ag alloyed nano-scale n-type Bi_2Te_3 based thermoelectric materials, Mater. Today Proc. **2** (2), 610-619 (2015). DOI: https://doi.org/10.1016/j.matpr.2015.05.083

[25] D.T. Morelli, V. Jovovic, and J.P. Heremans, Intrinsically minimal thermal conductivity in cubic I-V-VI2 semiconductors, Phys. Rev. Lett. **101** (3), 035901-1-035901-4 (2008). DOI: https://doi.org/10.1103/PhysRevLett.101.035901

[26] Q. Lognoné, F. Gascoin, Reactivity, stability and thermoelectric properties of n-Bi_2Te_3 doped with different copper amounts, J. Alloys Compd. **610**, 1-5 (2014). DOI: https://doi.org/10.1016/j.jallcom.2014.04.166

[27] R. Zybała, K. Kaszyca, M. Schmidt, M. Chmielewski, The properties of Bi_2Te_3-Cu joints obtained by SPS/FAST method, J. Electron. Mater. **48** (6), 3859-3865 (2019). DOI: https://doi.org/10.1007/s11664-019-07120-x

[28] E.A. Skrabek, D.S. Trimmer, CRC Handbook of Thermoelectrics, 1995 USA: CRC Press, New York.

[29] M. Fujikane, K. Kurosaki, H. Muta, S. Yamanaka, Electrical properties of α- and β-Ag_2Te, J. Alloys Compd. **387** (1-2), 297-299 (2005). DOI: https://doi.org/10.1016/j.jallcom.2004.06.054

[30] T. Ouyang, X. Zhang, M. Hu, Thermal conductivity of ordered-disordered material: A case study of superionic Ag_2Te, Nanotechnology 26 (**2**), 1-8 (2015). DOI: https://doi.org/10.1088/0957-4484/26/2/025702

[31] X. Zhang, L.-D. Zhao, Thermoelectric materials: Energy conversion between heat and electricity, J. Mater. **1** (2), 92-105 (2015). DOI: https://doi.org/10.1016/j.jmat.2015.01.001

[32] S. Lee, H.S. Shin, J.Y. Song, M.-H. Jung, Thermoelectric properties of a single crystalline Ag_2Te nanowire, J. Nanomater. **2017**, 4308968 (5 pages) (2017), DOI: https://doi.org/10.1155/2017/4308968

[33] M.H. Lee, J.-S. Rhyee, S. Kim, Y.-H. Choa, Thermoelectric properties of $Bi_{0.5}Sb_{1.5}Te_3/Ag_2Te$ bulk composites with size- and shape-controlled Ag_2Te nano-particles dispersion, J. Alloys Compd. **657**, 639-645 (2016). DOI: https://doi.org/10.1016/j.jallcom.2015.10.160

[34] T. Sakakibara, Y. Takigawa, K. Kurosawa, Hall mobility enhancement in $AgBiTe_2$-Ag_2Te composites, Jpn. J. Appl. Phys. **41** (5R), 2842-2844 (2002). DOI: https://doi.org/10.1143/JJAP.41.2842

[35] T. Sakakibara, Y. Takigawa, A. Kameyama, K. Kurosawa, Improvement of thermoelectric properties by dispersing Ag_2Te grains in $AgBiTe_2$ matrix: composition effects in $(AgBiTe_2)_{1-x}(Ag_2Te)_x$, J. Ceram. Soc. Japan **110** (4), 259-263 (2002). DOI: https://doi.org/10.2109/jcersj.110.259

[36] H. Fang, H. Yang, Y. Wu, Thermoelectric properties of silver telluride-bismuth telluride nanowire heterostructure synthesized by site-selective conversion, Chem. Mater. **26** (10), 3322-3327 (2014). DOI: https://doi.org/10.1021/cm501188c

[37] W.J. Parker, R.J. Jenkins, C.P. Butler, G.L. Abbott, Flash method of determining thermal diffusivity, heat capacity, and thermal conductivity, J. Appl. Phys. **32** (9), 1679-1684 (1961). DOI: https://doi.org/10.1063/1.1728417

[38] R.D. Cowan, Pulse method of measuring thermal diffusivity at high temperatures, J. Appl. Phys. **34** (4), 926-927 (1963). DOI: https://doi.org/10.1063/1.1729564

[39] J. I. Gersten, F. W. Smith, The Physics and Chemistry of Materials., 2001 John Wiley & Sons, INC., New York, USA.

[40] W. Gierlotka, Thermodynamic assessment of the Ag-Te binary system, J. Alloys Compd. **485** (1-2), 231-235 (2009). DOI: https://doi.org/10.1016/j.jallcom.2009.06.028

[41] O. Kubaschewski, C.B. Alcock, P.J. Spencer, Materials Thermochemistry, 6th ed. Oxford, 1993 Pergamon Press Ltd., New York.

[42] K.A. Borup, J. de Boor, H. Wang, F. Gascoin, X. Shi, L. Chen, M.I. Fedorov, E. Müller, B.B. Iversen, G.J. Snyder, Measuring thermoelectric transport properties of materials, Energy Environ. Sci. **8** (2), 423-435 (2015). DOI: https://doi.org/10.1039/C4EE01320D

[43] E.S. Toberer, M. Christensen, B.B. Iversen, G.J. Snyder, High temperature thermoelectric efficiency in $Ba_8Ga_{16}Ge_{30}$, Phys. Rev. B **77** (7), 075203-1-075203-8 (2008). DOI: https://doi.org/10.1103/PhysRevB.77.075203

[44] J. Zhang, X. Qin, D. Li, Ch. Song, Y. Liu, H. Xin, T. Zou, Y. Li, Optimized thermoelectric properties of $AgSbTe_2$ through adjustment of fabrication parameters, Electron. Mater. Lett. **11** (1), 133-137 (2015). DOI: https://doi.org/10.1007/s13391-014-4152-0

[45] B. Du, M. Liu, J. Xu, B. Hu, B. Liu, T. Su, J. Wang, Thermodynamic, structural and thermoelectric properties of $AgSbTe_2$ thick films developed by melt spinning, Nanomaterials-Basel **8** (7), 474 (10 pages) (2018), DOI: https://doi.org/10.3390/nano8070474

[46] L. Pan, D. Bérardan, N. Dragoe, High thermoelectric properties of n-Type $AgBiSe_2$, J. Am. Chem. Soc. **135** (13), 4914-4917 (2013), DOI: https://doi.org/10.1021/ja312474n

[47] A. Stegherr, P. Eckerlin, P. Wald, Untersuchung der Schnitte Ag_2Te-Bi_2Te_3 und $AgBiTe_2$-PbTe, Z. Metalkde. **54** (10), 598-600, (1963). DOI: https://doi.org/10.1515/ijmr-1963-541009

[48] https://www.asminternational.org/materials-resources/online-databases/-/journal_content/56/10192/15469013/DATABASE

[49] M.B. Babanly, Y.M. Shykhyev, N.B. Babanly, Y.A. Yusibov, Phase equilibria in the Ag-Bi-Te system, Russ. J. Inorg. Chem. **52** (3), 434-440 (2007). DOI: https://doi.org/10.1134/S0036023607030242

[50] I.A. Avramova, S.K. Plachkova, Electrical resistivity and scattering mechanisms of GeTe-rich thermoelectric materials in the system GeTe-$AgBiTe_2$, Phys. Status Solidi **179** (1), 171-177 (2000). DOI: https://doi.org/10.1002/1521-396X(200005)179:1<171::AID-PSSA171>3.0.CO;2-Z

[51] G. Tan, F. Shi, H. Sun, L.-D. Zhao, C. Uher, V.P. Dravidb, M.G. Kanatzidis, SnTe-$AgBiTe_2$ as an efficient thermoelectric material with low thermal conductivity, J. Mater. Chem. **A2** (48), 20849-20854 (2014). DOI: https://doi.org/10.1039/C4TA05530F

[52] J. de Boor, E. Müller, Data analysis for Seebeck coefficient measurements, Rev. Sci. Instrum. **84** (6), 065102-1-065102-0 (2013), DOI: http://doi.org/10.1063/1.4807697

[53] D.-H. Kim, T. Mitani, Thermoelectric properties of fine-grained Bi_2Te_3 alloys, J. Alloys Compd., **399** (1-2), 14-19 (2005). DOI: https://doi.org/10.1016/j.jallcom.2005.03.021

[54] J.W. Vandersande, A. Zoltan, C. Wood, Accurate determination of specific heat at high temperatures using the flash diffusivity method, Int. J. Thermophys. **10** (1), 251-257 (1989). DOI: https://doi.org/10.1007/BF00500723

[55] T.M. Tritt, Thermoelectric materials: Holey and unholey semiconductors, Science **283** (5403), 804-805 (1999). DOI: https://doi.org/10.1126/science.283.5403.804

[56] F.J. DiSalvo, Thermoelectric cooling and power generation, Science **285** (5428), 703-706 (1999). DOI: https://doi.org/10.1126/science.285.5428.703

[57] X. Tang, W. Xie, H. Li, W. Zhao, Q. Zhang, M. Niino, Preparation and thermoelectric transport properties of high-performance p-type Bi_2Te_3 with layered nanostructure, Appl. Phys. Lett. **90** (1), 012102 (2007). DOI: https://doi.org/10.1063/1.2425007

[58] L. Hu, T. Zhu, X. Liu, X. Zhao, Point defect engineering of high-performance bismuth-telluride-based thermoelectric materials, Adv. Funct. Mater. **24** (33), 5211-5218 (2014). DOI: https://doi.org/10.1002/adfm.201400474

[59] C.-H. Kuo, C.-S. Hwang, M.-S. Jeng, W.-S. Su, Y.-W. Chou, J.-R. Ku, Thermoelectric transport properties of bismuth telluride bulk materials fabricated by ball milling and spark plasma sintering, J. Alloys Compd. **496** (1-2), 687-690 (2010). DOI: https://doi.org/10.1016/j.jallcom.2010.02.171

[60] Y. Pan, T.-R. Wei, C.-F. Wu, J.-F. Li, Electrical and thermal transport properties of spark plasma sintered n-type $Bi_2Te_{3-x}Se_x$ alloys: the combined effect of point defect and Se content, J. Mater. Chem. C **3** (40), 10583-10589 (2015). DOI: https://doi.org/10.1039/C5TC02219C

[61] J. Jiang, L. Chen, S. Bai, Q. Yao, Q. Wang, Fabrication and thermoelectric performance of textured n-type $Bi_2(Te,Se)_3$ by spark plasma sintering, Mater. Sci. Eng. B **117** (3), 334-338 (2005). DOI: https://doi.org/10.1016/j.mseb.2005.01.002

[62] T. Zhu, L. Hu, X. Zhao, J. He, New insights into intrinsic point defects in V2VI3 thermoelectric materials, Adv. Sci. **3** (7), 1600004-1-1600004-16 (2016). DOI: https://doi.org/10.1002/advs.201600004

[63] T.S. Oh, D.-B. Hyun, N.V. Kolomoets, Thermoelectric properties of the hot-pressed $(Bi,Sb)_2(Te,Se)_3$ alloys, Scripta Mater. **42** (9), 849-854, (2000). DOI: https://doi.org/10.1016/S1359-6462(00)00302-X